Shear Jamming in Cornstarch

John Parker*
(Dated: June 1, 2015)

I. OVERVIEW

Granular materials exhibit the interesting property that, under some conditions, they behave like a solid (resists small stresses without deforming), while at other times they behave like a liquid (flows under an applied stress). The transition between these two phases is of physical interest.

One method to induce the phase transition is to change the packing fraction ϕ. This fraction is the ratio of the volume of material to the volume occupied – it measures how densely packed the material is. When the packing fraction is large enough, the grains interact strongly and form large force networks that can resist external stress. For $\phi > \phi_J$, the jamming fraction, the material behaves like a solid.

There exists another method to jam, even when $\phi < \phi_J$. By applying a large enough shear stress τ to the material, the state can become jammed. If too much shear stress is applied, the state becomes unjammed again. The precise nature of this jamming is not well understood [1].

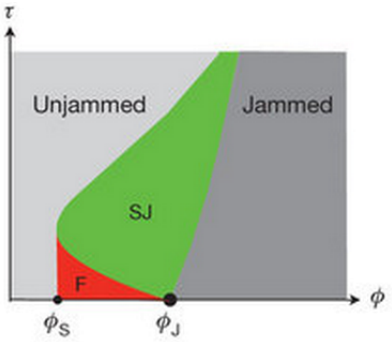

FIG. 1. Predicted phase space diagram for a granular material. A jammed state occurs due to a high packing fraction while shear jamming occurs due to an applied shear stress. The unjammed state has liquid-like properties. [1]

A dense suspension is created by mixing the grains with a liquid, such as when cornstarch is mixed with water. The result is a suspension that behaves like a liquid when undisturbed, but a solid-like mixture when external stresses are applied. The resulting solid is known to support normal stresses up to 1 mPa [2]. As the shear rate increases, the viscosity of the suspension also increases, a non-Newtonian property known as shear thickening. This property only occurs in some range of packing fractions — if the suspension is too dilute or dense, it does not occur.

This behavior is summed up in the phase space diagram of FIG. 1. There are three distinct regions: jammed states due to high packing fraction, shear jammed states due to shear, and unjammed states that behave like a liquid. While the behavior of the jammed and shear jammed states are known to be similar, their causes are quite different. This experiment is focused on the behavior of shear jammed cornstarch suspensions as the shear stress and packing fraction are varied.

A very defining solid-like behavior that the shear jammed cornstarch suspension exhibits is cracking. When the material is jammed, whether it be due to compression or shear, the resulting solid can crack and tear under additional stress,a behavior unknown to liquids. FIG. 2 shows several cracks forming in a cornstarch suspension as the center rod rotates. This rotation generates the shear stress needed to jam the suspension while the metal extrusions at the bottom of the rod (see FIG. 4) strike the suspension and cause it to crack.

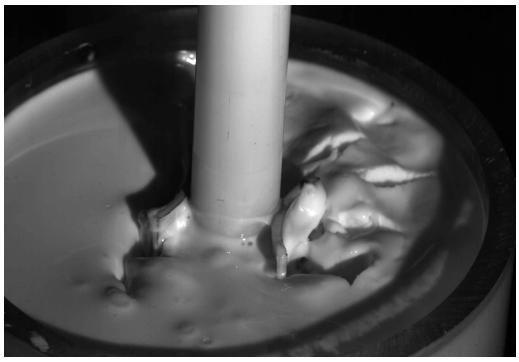

FIG. 2. An example of cracking in a dense suspension (the right portion of the container). The center rod and extrusion apply a shear stress that jams the suspension and causes it to exhibit the solid-like behavior of cracking.

This experiment explores the behavior of the solid phase of the cornstarch suspension, with an emphasis on the strength of the solid phase and the formation of cracks.

II. EXPERIMENTAL SETUP

The experimental setup in shown in FIG. 3. A DC motor is controlled by an external box with a motor controller nob. This number controls the frequency of rotation and power output of the motor. A belt connects

* Physics Department, University of Chicago

the motor to a metal shaft connected to another rod that dips into the cornstarch medium below. The container is designed to have an adjustable height so that the depth of the intruder can be controlled. An optical encoder (emits and receives IR signals) is placed with a picketed-fence wheel that rotates with the shaft. This allows measurement of the shaft frequency.

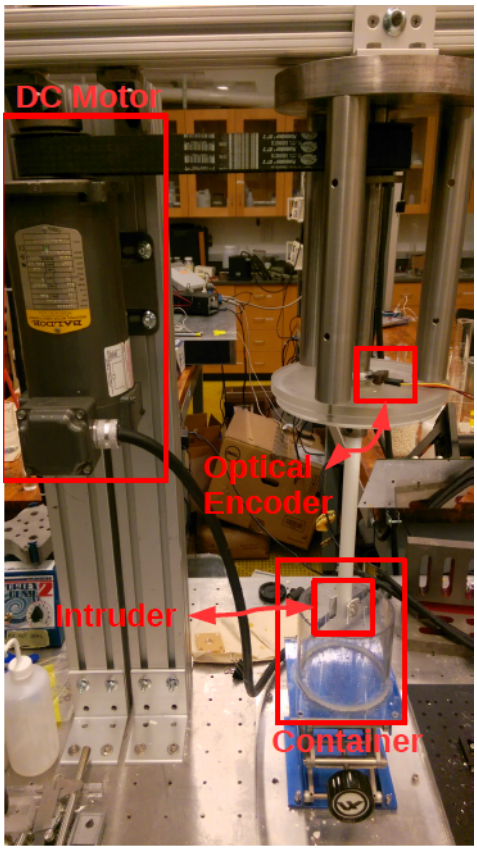

FIG. 3. Main components of the apparatus: A controlled motor rotates a shaft connected to the rod with extrusions (see FIG. 4). A container of adjustable height holds the cornstarch suspension. An optical encoder measures shaft frequency. A mirror reflects the cornstarch surface to a high-speed camera.

The intruder design is shown in FIG. 4. This design acts as four separate extrusions, each of which can cause cracks in the suspension.

A mirror is placed directly above the container at a 45° angle. This reflects the light from half of the cornstarch suspension surface and into a high-speed camera, which collects 6.38 seconds of video at 500 fps.

The cornstarch container has a diameter of 4.6 in. and height of 4.0 in. The intruding rod has diameter 0.75 in. with an extrusion of height 1.0 in. and width of 1.22 in.

The setup allows the measurement of the intruder rotation speed and images of the cornstarch surface. The control variables are the packing fraction of the suspension, ϕ, the motor controller number, and the depth of the intruder. In addition, glycerol can be added to the suspension to increase its viscosity (this necessity is explained in Appendix A)

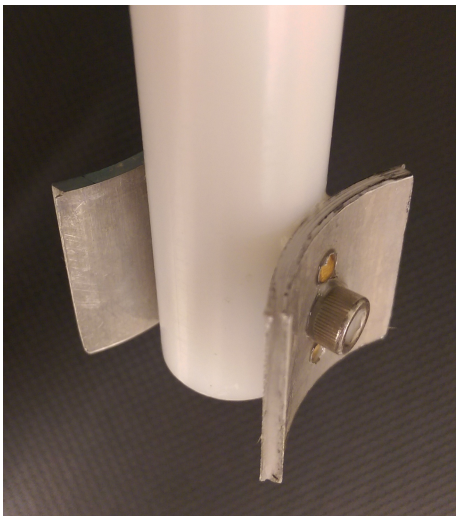

FIG. 4. The intruder used in this experiment to supply the shear stress and crack the suspension.

III. METHODS AND DATA

The packing fraction of the cornstarch suspension can be varied by controlling the ratio of cornstarch to water. The packing fraction is defined by

$$\phi = \frac{V_{cornstarch}}{V_{water} + V_{cornstarch}} \tag{1}$$

Using the densities of cornstarch and water, the packing fraction can be determined from the masses of each component. A more detailed account is given in Appendix A, including uncertainties and known issues.

For measuring the frequency, the motor controller nob is initially turned to the desired value and the break switch is thrown on (this starts/stops the motor as quickly as possible). Data collection from the optical encoder begins, and then the break is turned off. This allows measurement of the build-up in frequency. Appendix B explains the process of turning the encoder output into a frequency.

The depth of the intruder, h, is controlled with the height of the container. The lowest depth of interest is the height of the intruder, $h = 1$ in.

When the suspension is seen to exhibit cracks (which occur only for certain ϕ and angular speed), video footage of the surface is taken.

A. Frequency Data

Frequency data was collected in the absence of any medium (that is, in air). This allows an understanding of how the motor varies with the controller number

under negligible stress. Frequency data collected in the presence of a medium is then compared to this response.

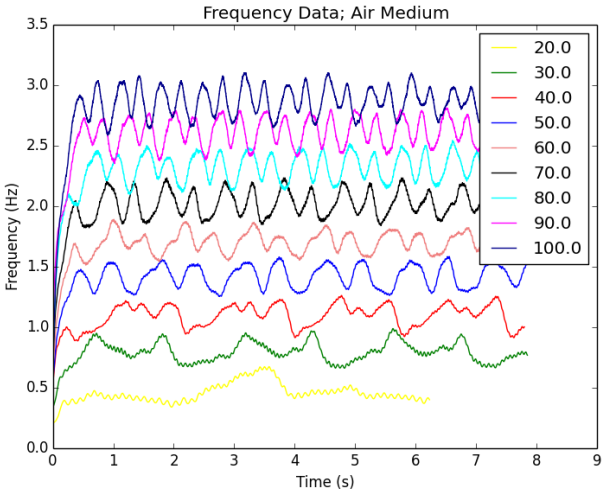

FIG. 5. The optical encoder allows measurement of the shaft frequency. This is done in the absence of any medium (in air). A range of motor controller values are swept (20 through 100) and the frequency over time is extracted. $t = 0$ corresponds to the motor being turned on.

FIG. 5 shows the motor's frequency response from a given controller number (varied from 20 to 100). $t = 0$ corresponds to the time at which the break is turned off. There is about a 0.5 s build-up before a steady oscillation occurs. The motor does not apply a steady rotation, but there is an increase of the average final frequency with the control number.

FIG. 16 of Appendix C shows the Fourier transform of these frequency curves and discusses the small oscillations occurring around the average. The frequency from now on is taken to be the average of the oscillation, and there is an uncertainty given by the oscillation's standard deviation, $f = f_{avg} \pm \sigma_{osc}$.

The same results for a water medium are shown in FIG. 15 of Appendix C. The results are very similar, as is demonstrated in FIG. 8.

The cornstarch medium is also used while collecting frequency data. The results of a particular experiment are shown in FIG. 6, with $\phi = 41\%$ and intruder depth $h = 1$ in. This data is collected for various ϕ and depths. The average frequencies are lower than in the absence of a medium (or water) and there is often a longer build-up.

When glycerol is added to the suspension, the typical frequency outputs are shown in FIG. 7. The results are quite different from the regular cornstarch suspension. There is a period of time in which the motor is turned on and stuck before the frequency shoots up to its final value. The onset time, t_c, is defined as the amount of time required for the motor to reach its final frequency. This is seen to decrease with increasing control number. For those that remain stuck, the onset time is set to $t_c = \infty$.

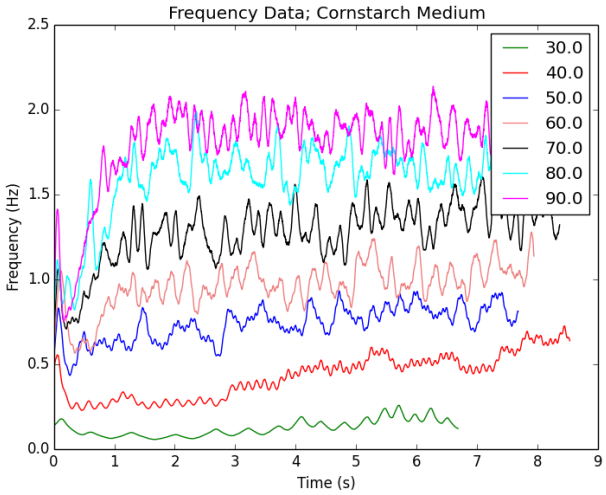

FIG. 6. The same frequency measurement done with the intruder in cornstarch. The average frequencies are lower (see FIG. 8) and noisier. They also have a different buildup behavior from $t = 0$.

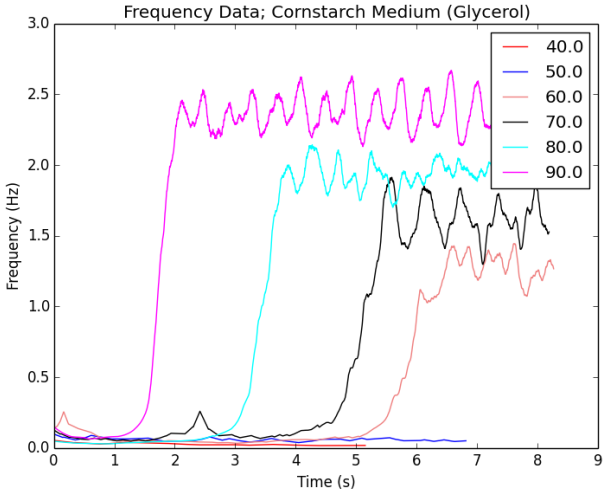

FIG. 7. The frequency measurement for a cornstarch medium with glycerol. The motor gets stuck for a period of time before cracking the suspension and jumping up in speed.

The role of glycerol and the higher ϕ values are discussed further in Appendix A.

B. Suspension Strength

The strength of each suspension can be measured based on the frequency response of the medium at a given control number. FIG. 8 shows the final frequency of the shaft against increasing control number for the cornstarch suspension. The air and water medium overlap and provide an upper limit on all of the other curves.

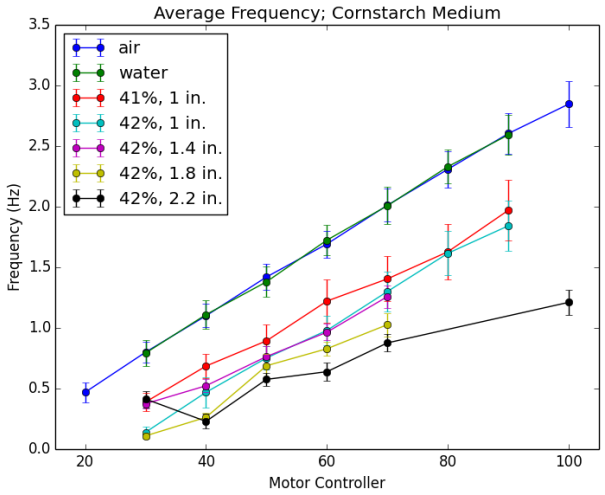

FIG. 8. The average frequency varies with the motor controller. The air/water medium provide an upper limit. Higher packing fractions or deeper depths hinder the motor's rotation, implying a stronger suspension.

Each curve is approximately linear, so the frequency increases in the expected way with control number. The actual values and slopes of these lines decrease with increasing packing fraction (from 41% to 42%) and also with increasing depth. This suggests that the medium is stronger when deeper into the suspension. This behavior may be due to separation of cornstarch and water over time due to their different densities (discussed further in Appendix A). The gravitational force can cause the suspension to have a ϕ that increases with increasing depth.

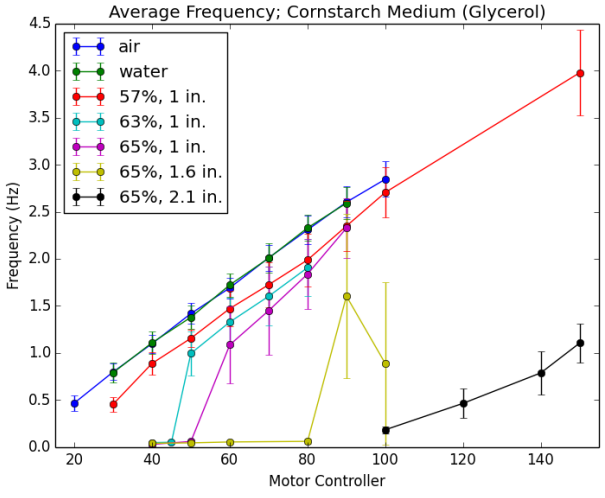

FIG. 9. Average frequencies for a cornstarch medium with glycerol. The onset time for rotation to occur is seen to increase with packing fraction or depth.

Similar curves are shown for the cornstarch suspensions with glycerol in FIG. 9. The glycerol is added in an attempt to reduce the separation of colloid and liquid over time by increasing the viscosity of the suspension. The results for these suspensions become non-linear during the lower control numbers where the motor strains too much to maintain any frequency. At some value, the frequency shoots up as the intruder cracks and breaks through the suspension. The values are again lower with increasing ϕ and depth.

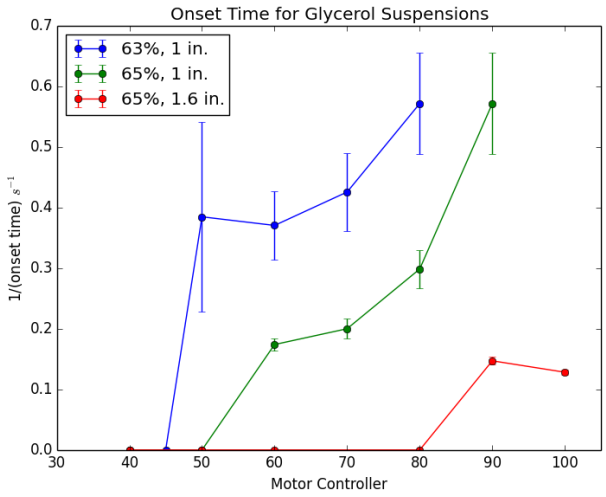

FIG. 10. The onset time for the glycerol suspensions decreases with increasing motor controller. $1/t_c$ is plotted so that infinite onset times can converge.

From FIG. 7, the onset time at a given control number can be extracted. FIG. 10 plots $1/t_c$ for two different suspensions and one at a larger depth. Plotting the inverse allows the $t_c = \infty$ values to converge. Higher packing fractions and larger depths have a higher onset times.

C. Crack Formation

In the glycerol suspensions with $\phi = 63\%$, 65%, the suspension does not respond to low control numbers. When the driving force gets large enough, the onset time becomes finite. Video footage of the cornstarch surface indicates that this onset time coincides with the formation of a crack.

FIG. 11 shows the formation of a crack at $\phi = 63\%$, $h = 1$ in., and a motor control number 55. From FIG. 9, this corresponds to the cyan curve just after a finite onset time can occur. The crack starts from the center of the container and propagates radially outward, reaching its full length in around 0.88 seconds.

A crack of this nature was a relatively rare event and only occurred around this value of ϕ. Three separate videos of different cracks were obtained at this packing fraction and control number. FIG. 12 plots the length

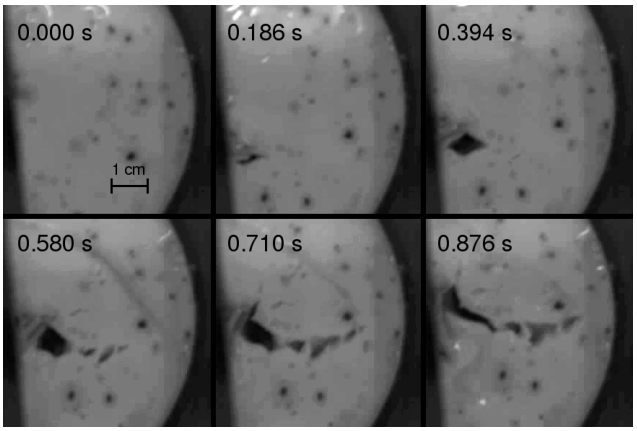

FIG. 11. The evolution of a crack in a glycerol suspension. $\phi = 63\%$ and the motor controller was set to 55.

of the crack versus time for the three cracks. These repeated measurements suggest that the cracks propagate at a speed of about 3 cm/s.

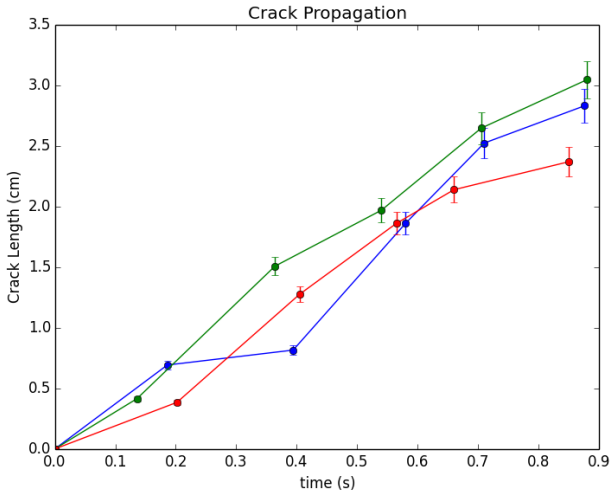

FIG. 12. The length of three different cracks versus time. $\phi = 63\%$ and the motor controller was set to 55 for each crack observed.

Afterwards, the crack disappears and the intruder spins at a much higher frequency. The suspension's high viscosity prevents it from settling in a volume around the intruder, which now acts like a repulsive barrier. No more cracks are then observed.

IV. FINAL REMARKS

This experiment focused on the solid phase of dense cornstarch suspensions and measuring material strength and crack properties. There are many other areas of interest to explore and improve upon in these experiments, discussed below.

The packing fraction in these experiments are subject to local fluctuations which make it very difficult to characterize and control the medium. The best way to overcome this issue is to density match the water and cornstarch by mixing CsCl in with the water. This would prevent the separation of water and colloid over time, and may prevent the need of glycerol.

A more useful quantity to use instead of the (average) shaft frequency or motor controller number would be the applied shear stress, as it is this stress that causes the medium to jam and crack. This could possibly be achieved by attaching force sensors to the rod and intruder.

Finally, a deeper analysis of crack properties would be insightful. How these crack properties vary with different applied shear stresses or different packing fractions would help further characterize them. In addition, the actual size and shape of the intruder causing the cracks could be changed.

APPENDIX A: MEASURING ϕ

There are inherent uncertainties in measuring the packing fraction exactly. Cornstarch in an open container absorbs moisture from the room, so the exact water content is left unknown. Based on previous measurements, the typical fraction of cornstarch mass to water mass is $\eta = 0.9 \pm .03$. When mixing the cornstarch and water, some known mass of water, M_w, and mass of cornstarch, M_c, are mixed together. The equation for ϕ becomes

$$\phi = \frac{\eta M_c/\rho_c}{\eta M_c/\rho_c + (1-\eta)M_c/\rho_w + M_w/\rho_w} \qquad (2)$$

where $\rho_c = 1.625\ g/cm^3$ and $\rho_w = 1.00\ g/cm^3$ are the respective densities of cornstarch and water.

When glycerol is added to the system, it contributes an additional term in the denominator, M_g/ρ_g, where $\rho_g = 1.26\ g/cm^3$. The glycerol suspensions tend to have higher packing fractions, as seen in section III.A.

Glycerol is used to help prevent a problem that occurs in the regular cornstarch suspensions. At higher packing fractions or after about 10 minutes have passed since mixture, the suspension begins to separate. Section III demonstrated a packing fraction that varied with the height. In addition, it is possible to have a radially varying packing fraction after the intruder has been rotating for a while.

FIG. 13 shows an example of this happening. The experiment was done over a period of 10 minutes at $\phi = 43\%$. Afterwards, the center became liquid-like while the outer radius became solid-like. Since higher packing fractions were needed to crack the suspension, a switch to glycerol was needed to observe cracks. The problem depicted here did not occur with the glycerol mixtures.

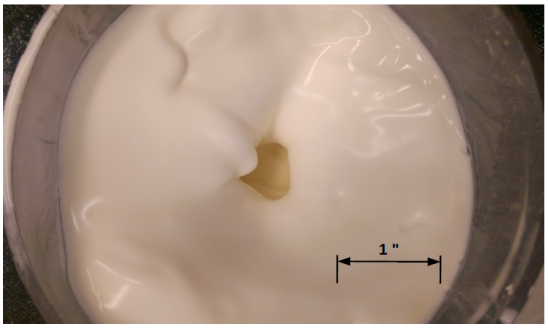

FIG. 13. An example of the non-glycerol suspension having a radially varying packing fraction ϕ. Outside the inner radius, the suspension is jammed without any shear.

APPENDIX B: MEASURING FREQUENCY

The optical encoder shown in FIG. 3 produces a voltage output proportional to the intensity of the IR signal it receives. As the code-wheel spins with the shaft, the voltage varies from zero to nonzero voltage in a periodic fashion. The actual output of the encoder over a tenth of a second is shown in FIG. 14.

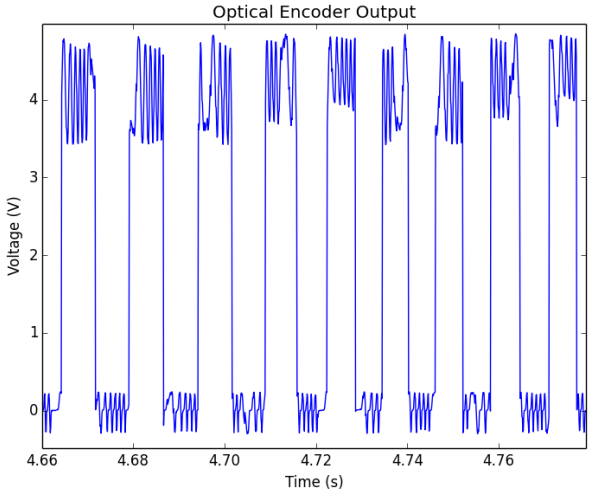

FIG. 14. The raw data output of the optical encoder. The width of each step indicates the time required for 1/200 of a cycle. The frequency vs time plots (such as FIG. 15) can be extracted from this data by averaging the times over a few steps and iterating though the data.

Each voltage step corresponds to 1/200 of a cycle. By measuring the width of each step, the average frequency over that time period can be extracted. To get a cleaner response, the frequency is averaged over a few periods of the signal. Doing this over the whole signal allows the construction of a frequency vs. time plot (those shown in III.A)

APPENDIX C: ADDITIONAL DATA

FIG. 15 shows the frequency-time plot for water, which isn't much different than the response in air. This was done to show that the cornstarch suspension is not just a simple fluid like water.

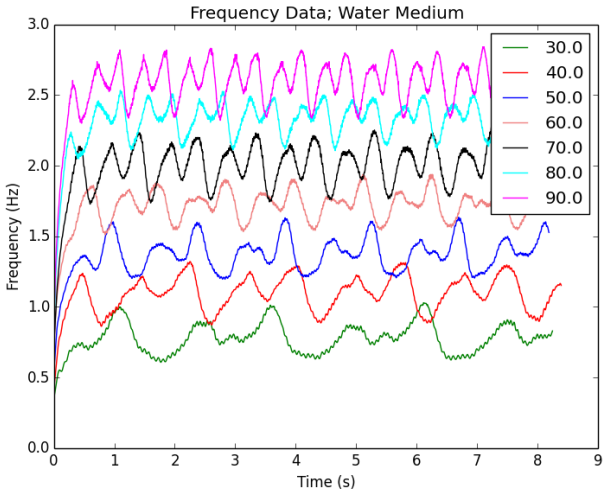

FIG. 15. The frequency output of the optical encoder in a water suspension. The result is nearly identical to the air medium (see FIG. 8). This demonstrates the non-Newtonian behavior seen earlier with the cornstarch suspensions.

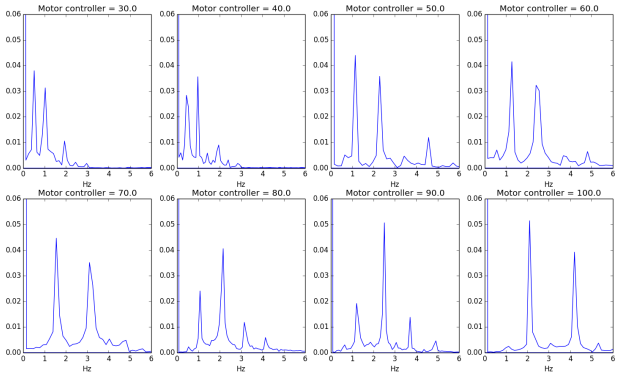

FIG. 16. The Fourier transform of the various curves from FIG. 5. This indicates that the motor supplies two dominant frequencies on top of a uniform rotation. These frequencies increase with increasing motor controller number.

FIG. 16 is the Fourier transform of the air frequencies of FIG. 5. The frequency has three peaks in its spectrum. One of these is the zero frequency corresponding to uniform rotation. The remaining two correspond to small oscillations of the frequency around the average. The motor supplies these frequencies without any load, and appear to be a part of its operation. Moreover, the

two frequencies increase with increasing motor controller number. These oscillations generate extra noise in the system, but not so much that different average frequencies cannot be distinguished.

ACKNOWLEDGMENTS

I would like to give special thanks to Heinrich Jaeger and Ivo Peters, as well as the rest of the Jaeger Group, for their help and insight with this project.

[1] Dapeng Bi, Jie Zhang, Bulbul Chakraborty, and RP Behringer. Jamming by shear. *Nature*, 480(7377):355–358, 2011.

[2] Eric Brown and Heinrich M Jaeger. Shear thickening in concentrated suspensions: phenomenology, mechanisms and relations to jamming. *Reports on Progress in Physics*, 77(4):046602, 2014.

[3] Matthieu Roché, Eglind Myftiu, Mitchell C Johnston, Pilnam Kim, and Howard A Stone. Dynamic fracture of nonglassy suspensions. *Physical review letters*, 110(14):148304, 2013.